Transient response of magnetorheological elastomers to step magnetic field

Qianqian Wen, Yu Wang, Jiabin Feng, and Xinglong Gong

Citation: Appl. Phys. Lett. **113**, 081902 (2018); doi: 10.1063/1.5048368
View online: https://doi.org/10.1063/1.5048368
View Table of Contents: http://aip.scitation.org/toc/apl/113/8
Published by the American Institute of Physics

Transient response of magnetorheological elastomers to step magnetic field

Qianqian Wen, Yu Wang,[a] Jiabin Feng, and Xinglong Gong[a]
CAS Key Laboratory of Mechanical Behavior and Design of Materials, Department of Modern Mechanics, University of Science and Technology of China, Hefei 230027, People's Republic of China

(Received 13 July 2018; accepted 7 August 2018; published online 21 August 2018)

The time-dependent performance of magnetorheological elastomers (MREs) under a magnetic field is important for the precise control of smart devices based on MREs. Here, the transient responses of anisotropic magnetorheological elastomers, including magnetic field-induced storage modulus ($\Delta G'$) and loss modulus ($\Delta G''$), were investigated under different step magnetic fields. The results indicated that $\Delta G'$ increased over time while $\Delta G''$ decreased after the initial jump in the loading stage of the step field. $\Delta G'$ quickly dropped to 0, while $\Delta G''$ continued to decrease gradually in the removal stage of the step field. A comprehensive model based on magnetic dipolar and viscoelastic parameter models was proposed to explain the transient responses. *Published by AIP Publishing.*
https://doi.org/10.1063/1.5048368

Magnetorheological elastomers (MREs) are composites which consist of micro-sized magnetizable particles embedded into a non-magnetizable polymer matrix. Their many properties, such as stiffness, viscosity, magnetostriction, and electrical conductivity, can be controlled by an external magnetic field.[1–4] At present, MREs have been widely applied in various smart devices such as vibration absorbers,[5,6] vibration isolators,[7,8] and sandwich beams.[9,10]

In most MRE-based devices, the step magnetic field was employed to achieve rapid and controllable stiffness.[11,12] Therefore, it is very important to study the transient response of MREs for the precise control of the MRE-based devices. However, most of the previous studies focused on the magnetic field-dependent behaviors of MREs in the steady state.[13,14] The time-dependent properties of MREs in the unstable state were rarely studied. The existing research studies have shown that the transient magnetorheological response of MREs was mainly due to the restructuring of the ferromagnetic filler after step magnetic field perturbation.[15–17] However, a phenomenological multiple-exponential model was proposed to describe the transient response of MREs under the step magnetic field in previous studies. There is still a lack of knowledge on the correlation between the microstructural evolution and the transient response of MR materials.

In this study, the magnetic field-induced storage modulus ($\Delta G'$) and loss modulus ($\Delta G''$) of anisotropic MREs under different step magnetic fields were investigated. A comprehensive model based on the magnetic particles' rearrangement was proposed to explain their transient magnetorheological response. The MRE samples were fabricated with carbonyl iron particles (Type CN, BASF Co., Germany), Polydimethylsiloxane, and curing agent (Sylgard 184, Dow Corning GmbH, USA). The anisotropic MRE samples were cured at 90 °C for 20 min under a pre-structure magnetic field of 1.5 T. The mass fraction of carbonyl iron particles was 50 wt. %. The shear storage modulus and loss modulus of MREs were measured using a plate-plate magneto-rheometer (Physica MCR 302, Anton Paar Co., Austria). The sample size was 20 mm in diameter and 1 mm in thickness. The measurement was conducted in an oscillating mode with a constant strain amplitude of 0.1%, a frequency of 5 Hz, a pre-pressure force of 10 N, and a temperature of 25 °C.

Figures 1(a) and 1(b) show the time dependences of $\Delta G'$ and $\Delta G''$ of the anisotropic MREs under different step magnetic fields. The results showed that $\Delta G'$ and $\Delta G''$ remained around 0 in the absence of the magnetic field ($-50 < t < 0$ s). This indicated that the storage and loss modulus of MREs were independent of time when $B = 0$. When the step magnetic field was applied ($0 < t \leq 100$ s), $\Delta G'$ increased rapidly at first and then gradually stabilized, while $\Delta G''$ started to decrease rapidly after the initial jump and then gradually stabilized. After the step magnetic field was removed ($t > 100$ s), $\Delta G'$ rapidly dropped to 0, while $\Delta G''$ still increased rapidly at first and then gradually stabilized. The magnetic field-induced property changes of MREs were mainly determined by the magnetic properties and microstructure of the particles. Previous studies had indicated that particles within the anisotropic MREs did not exhibit an ideal straight-chain structure along the direction of the pre-structure magnetic field.[18–20] In this experiment, the measured scanning electron microscopy (SEM) images of the sample also proved it. Figure 1(c) shows the chain-like structure in the MREs along the direction of the pre-structural magnetic field. However, a more sophisticated image [Fig. 1(d)] shows that the internal particles were not ideal straight-chain structure but a wavy-chain structure. Thus, the resulting interaction forces between the particles due to the magnetic polarization under the external field would prompt the linearization of the wavy-chain structure [Fig. 2(a)]. The transient response of the MREs under step magnetic field perturbation was definitely related to the restructuring process of the filler particles.

A comprehensive model was proposed here to describe the transient response of MREs under the step magnetic field. On the microscale, the proposed composite material consisted of a polymeric matrix with embedded magnetizable

[a]Authors to whom correspondence should be addressed. wyu@ustc.edu.cn and gongxl@ustc.edu.cn

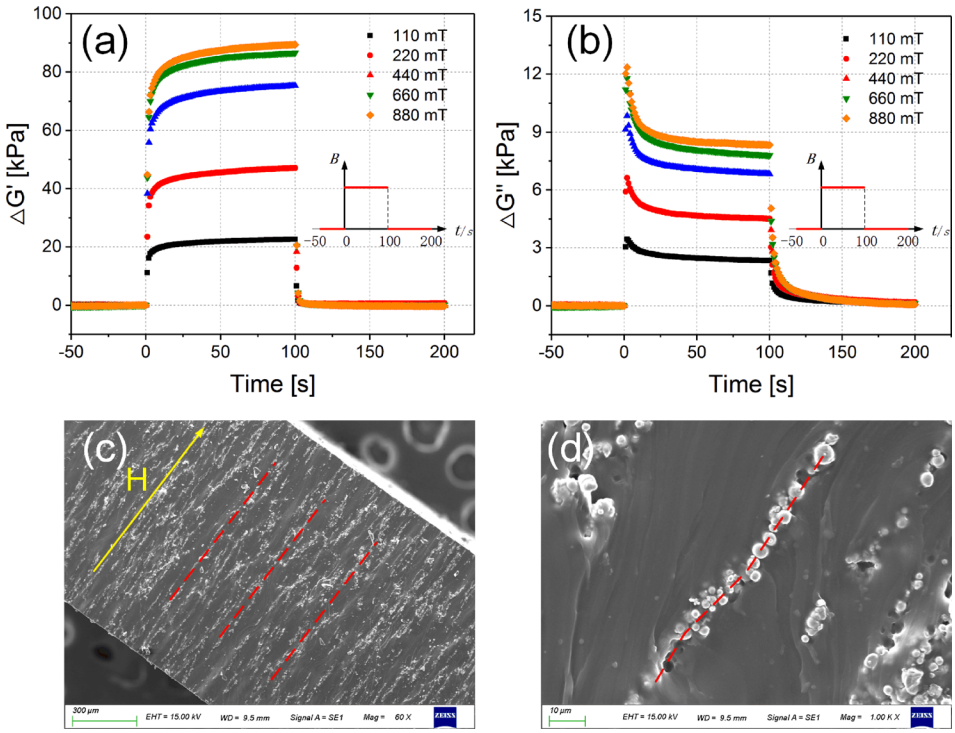

FIG. 1. Time dependences of (a) $\Delta G'$ and (b) $\Delta G''$ for the anisotropic MREs under different step magnetic fields. The inset shows the way of the step magnetic field loading. SEM images of the anisotropic MREs (c) at 60× magnification and (d) at 1000× magnification.

particles as shown in Fig. 2(a). The considered idealized two-dimensional microstructure is shown in Fig. 2(b). Its internal structure was motivated by the wavy-chain arrangement of magnetization particles, as shown in Fig. 1(d), which was formed due to the particle interaction during the curing process of the composite's polymeric matrix with an applied magnetic field. The representative volume element (RVE) in Fig. 2(b) contained three circular particle inclusions. For the neighboring particles 1 and 2 in the wavy-chain structure, the magnetostatic energy between the two particles is[21]

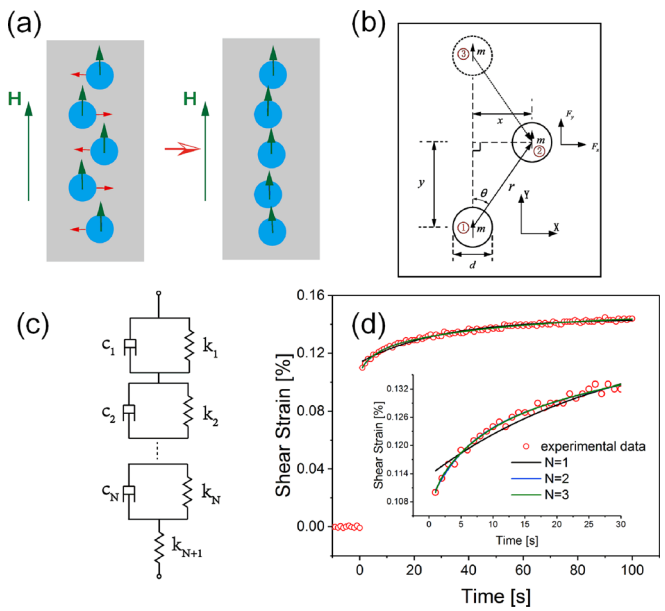

FIG. 2. (a) The schematic diagram of particles' movement. The red and green arrows indicate the direction of particle's movement and magnetization, respectively. (b) The magnetic dipolar model of MREs. (c) Generalized parameter model of viscoelastic materials. (d) The shear strain of MREs' matrix under a step shear stress of 100 Pa at t = 0, fitted by prony series with different N.

$$E_{12} = \frac{m^2(1-3\cos^2\theta)}{4\pi\mu_1\mu_0 r^3} = \frac{m^2(x^2-2y^2)}{4\pi\mu_1\mu_0(x^2+y^2)^{5/2}}, \quad (1)$$

where m is the dipole moment, $r\,(=\sqrt{x^2+y^2})$ is the inter-particle distance, θ is the angle between the line connecting the two dipoles and the direction of magnetization, μ_0 is the permeability of vacuum, and μ_1 is the relative permeability of the matrix. The magnetic dipole interaction is

$$F_x = -\frac{\partial E_{12}}{\partial x}\bigg|_{y=y_0} = \frac{3m^2}{4\pi\mu_1\mu_0 {y_0}^4} \times \frac{s(s^2-4)}{(1+s^2)^{7/2}}, \quad s = \frac{x}{y_0}, \quad (2)$$

where y_0 is the inter-particle distance in the direction of m. The magnetic field-induced transverse stiffness is

$$K_x = \frac{\partial^2 E_{12}}{\partial x^2}\bigg|_{y=y_0} = \frac{3m^2}{4\pi\mu_1\mu_0 {y_0}^5} \times \frac{(4+4s^4-27s^2)}{(1+s^2)^{9/2}}, \quad s = \frac{x}{y_0}, \quad (3)$$

where $s\,(=x/y_0)$ is defined as the transverse geometric characteristic parameter of the wavy-chain structure. When the anisotropic MREs [Fig. 2(b)] ($s < 0.4$) were applied with a step magnetic field, driven by negative magnetic interaction force F_x, the particles tended to move along the negative X direction to make the wavy structure linearization. Moreover, with decreasing s, F_x decreased and K_x increased [see Fig. S2]. It could explain why the stiffness increased over time after the step field was loading.

The matrix of MREs is generally a polymer, which is a typical viscoelastic material. To clarify the time-dependent characteristic of the particles' movement, a generalized prony series viscoelastic parameter model [Fig. 2(c)] was adopted here

$$\varepsilon(t) = \sigma_0 J_N(t) = \sigma_0\left(\sum_{n=1}^{N+1}\frac{1}{k_n} - \sum_{N=1}^{N}\frac{1}{k_n}e^{-\frac{t}{\tau_n}}\right)$$

$$= A_0 - \sum_{N=1}^{N} A_n e^{-\frac{t}{\tau_n}}, \quad (4)$$

where $A_0 = \varepsilon_t(t \to \infty)$, A_n, and τ_n are the amplitude and the characteristic time of the nth process, respectively. The number (N) of Kelvin element models is related to the viscoelastic properties of the matrix material. Therefore, the N for different matrices may be different, depending on the viscoelastic properties of the MRE matrix. The creep experiment of MREs under zero magnetic field was conducted, and the data were fitted by prony series with different N [Fig. 2(d)]. Obviously, the fitting curve (N = 1) deviated from the experimental data in the initial stage of creep. Both the curves of N = 2 and N = 3 fitted the experimental data very well and the two curves were almost coincident, which indicated that the parameter model with minimum N = 2 could characterize the matrix's viscoelastic properties well.

Based on the above analyses of the magnetic dipole interaction with the wavy chain structure and the viscoelastic properties of the MREs' matrix, the proposed comprehensive model of MREs is shown in Fig. 3(a). The particle aggregates tended to be straight when the step field was applied (indicated by the red arrow) and then returned to the initial position after the step field was removed (indicated by the black arrow). According to this model, the particle's movement in the loading stage (Δx_l) and removal stage (Δx_r) can be expressed as a double-exponential function

$$\Delta x_l(t) = A_0 - A_1 e^{-\frac{t}{\tau_1}} - A_2 e^{-\frac{t}{\tau_2}}, \tag{5}$$

$$\Delta x_r(t) = B_0 + B_1 e^{-\frac{t}{\tau_{1n}}} + B_2 e^{-\frac{t}{\tau_{2n}}}, \tag{6}$$

where τ_1, τ_2, τ_{1n}, and τ_{2n} are the characteristic times of particle's movement, and A_n and B_n (n = 0, 1, 2) are the positive weight of each exponential function term [see Eq. (S15)]. The characteristic times indicated how fast the internal particles reach the equilibrium position. A smaller characteristic time means a shorter time for the particle to arrive at the equilibrium position.

From the time-dependent particles' movement, the expression of $\Delta G''(t)$ and $\Delta G'(t)$ under the step magnetic field could be given. $\Delta G''$ depended on the increased frictional loss between particles and the matrix compared to the zero-field condition. When the step magnetic field was applied, because of the magnetic dipole interaction, the relative displacement of particles and the matrix was limited. It is assumed that the friction is proportional to the magnetic dipole interaction during the movement. Therefore, $\Delta G''$ in the load stage ($\Delta G_l''$) was mainly related to the increased interaction between the matrix and the particles

$$s_l(t) = \frac{x}{y_0} = \frac{x_0 - \Delta x_l(t)}{y_0} = \frac{1}{y_0}\left[(x_0 - A_0) + A_1 e^{-\frac{t}{\tau_1}} + A_2 e^{-\frac{t}{\tau_2}}\right], \tag{7}$$

$$\Delta G_l''(t) \propto |F_x| = \frac{3m^2}{4\pi\mu_1\mu_0 {y_0}^4} \times \frac{s_l({s_l}^2 - 4)}{(1 + {s_l}^2)^{7/2}} \approx \frac{3m^2}{\pi\mu_1\mu_0 {y_0}^4} \times s_l \propto C_0 + C_1 e^{-\frac{t}{\tau_1}} + C_2 e^{-\frac{t}{\tau_2}}, \tag{8}$$

where the approximation ignores the second and higher-order terms of the Taylor series expansions. After the step magnetic field was removed, the magnetic dipole interaction rapidly disappeared and the relative displacement of particles and the matrix was not limited. Therefore, $\Delta G''$ in the removal stage ($\Delta G_r''$) was related to the increased free movement of the particles in the matrix

$$\Delta G_r''(t) \propto \Delta x_r(t) = B_0 + B_1 e^{-\frac{t}{\tau_{1n}}} + B_2 e^{-\frac{t}{\tau_{2n}}}. \tag{9}$$

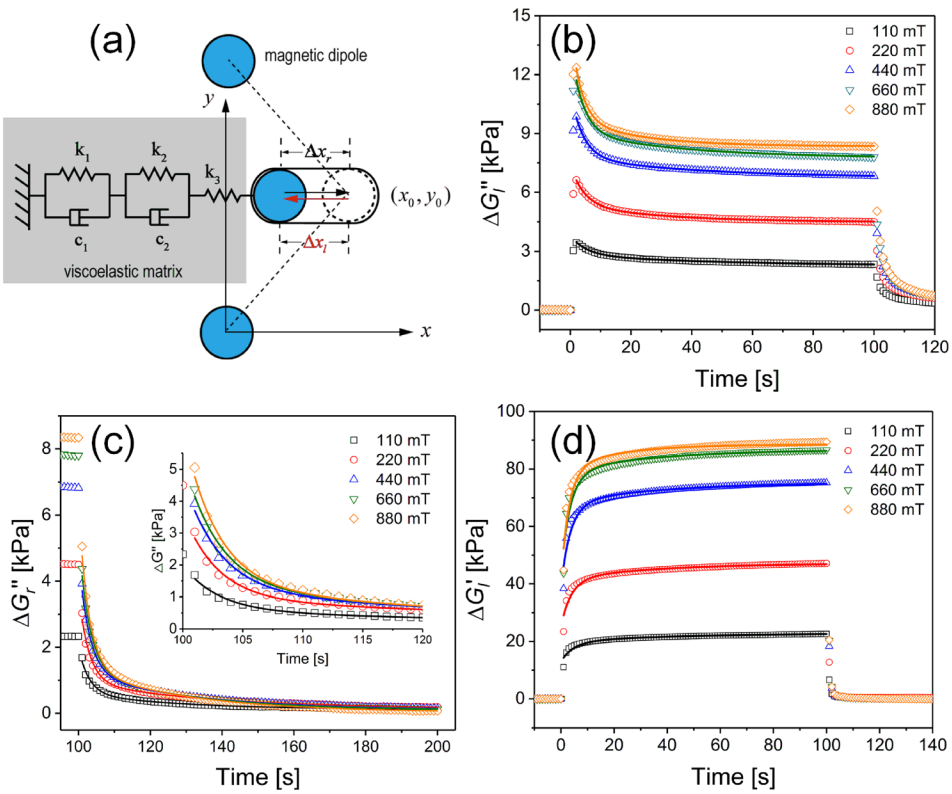

FIG. 3. (a) The comprehensive model based on magnetic dipolar and viscoelastic parameter models of MREs. Fitting results of (b) $\Delta G_l''$ in the loading stage; (c) $\Delta G_r''$ in the removal stage; (d) $\Delta G_l'$ in the loading stage. Hollow symbols represent the experimental data, and the solid lines represent the fitting curves.

TABLE I. Fitting results of the characteristic time.

B (mT)	τ_1 (s)	τ_2 (s)	τ_{1n} (s)	τ_{2n} (s)
110	5.29	49.2	2.89	28.6
220	4.36	40.3	2.81	36.7
440	4.02	38.9	2.96	31.2
660	3.82	35.4	2.93	28.6
880	3.36	21.8	2.82	29.7

Both $\Delta G_l'$ ($\Delta G'$ in the loading stage) and $\Delta G_r'$ ($\Delta G'$ in the removal stage) were determined by the field-induced stiffness

$$\Delta G_l'(t),\ \Delta G_r'(t) \propto K_x \approx \frac{3m^2}{4\pi\mu_1\mu_0 y_0{}^5} \times (4 - 45s^2)$$
$$\propto D_0 - D_1\left(C_0 + C_1 e^{-\frac{t}{\tau_1}} + C_2 e^{-\frac{t}{\tau_2}}\right)^2, \quad (10)$$

where the approximation ignores the three and higher-order terms of the Taylor series expansions. After the magnetic field was removed, m rapidly dropped to 0, causing $\Delta G_r'$ rapidly decrease to zero as shown in Fig. 1(a). In summary, $\Delta G_l''$, $\Delta G_r''$, and $\Delta G_l'$ all have the exponential function forms as expressed in Eqs. (8)–(10), respectively.

Figures 3(b)–3(d) show the fitting results of $\Delta G_l''$, $\Delta G_r''$, and $\Delta G_l'$. It is seen that the experimental data were fitted very well by the model. Table I lists the fitting parameters of the characteristic time. Based on the derivation from the proposed model [see Sec. 2 in the supplementary material], the characteristic time in the field loading stage (N = 1)

$$\tau = \frac{c_1}{k_1 + \left(k_m{}^{-1} + k_2{}^{-1}\right)^{-1}}, \quad \text{where } k_m = \frac{3m^2}{\pi\mu_1\mu_0 y_0{}^5}, \quad (11)$$

which was negatively correlated with the magnetic field, and the characteristic time in the field removal stage (N = 1)

$$\tau_n = \frac{c_1}{k_1}, \quad (12)$$

which was only related to the viscoelastic properties of the matrix. As shown in Table I, τ_1 and τ_2 decreased with the increase in the magnetic field, while τ_{1n} and τ_{2n} were basically unchanged with different magnetic fields. These results indicated that the change trends of the fitting characteristic time were in accordance with the expectation from the proposed model well.

In conclusion, the transient dynamic responses ($\Delta G'$ and $\Delta G''$) of anisotropic MREs under different step magnetic fields were investigated. The change trends of $\Delta G'$ and $\Delta G''$ over time showed a strong "viscoelastic" characteristic. These trends were attributed to the restructuring of the magnetic filler particle. The magnetic dipole interaction of the wavy chain structure and the viscoelastic properties of the matrix would finally affect the characteristic time of the movement. The characteristic time in the field loading stage decreased with the increase in the step magnetic field, while the characteristic time in the field removal stage remained basically unchanged with the step magnetic field.

See supplementary material for the characteristic of the magnetic dipole interaction and influence of the step magnetic field on the characteristic times.

Financial support from the National Natural Science Foundation of China (Grant No. 11572309) and the Strategic Priority Research Program of the Chinese Academy of Sciences (Grant No. XDB22040502) is gratefully acknowledged. This work was also supported by the Collaborative Innovation Center of Suzhou Nano Science and Technology.

[1]J. D. Carlson and M. R. Jolly, Mechatronics **10**, 555 (2000).
[2]I. Bica, Mater. Lett. **63**, 2230 (2009).
[3]R. Li and L. Z. Sun, Appl. Phys. Lett. **99**, 131912 (2011).
[4]M. Yu, S. Qi, J. Fu, and M. Zhu, Appl. Phys. Lett. **107**, 111901 (2015).
[5]A. A. Lerner and K. A. Cunefare, J. Intell. Mater. Syst. Struct. **19**, 551 (2008).
[6]S. S. Sun, H. X. Deng, J. Yang, W. H. Li, H. P. Du, G. Alici, and M. Nakano, Smart Mater. Struct. **24**, 045045 (2015).
[7]W. H. Li, X. Z. Zhang, and H. P. Du, J. Intell. Mater. Syst. Struct. **23**, 1041 (2012).
[8]Y. C. Li, J. C. Li, T. F. Tian, and W. H. Li, Smart Mater. Struct. **22**, 095020 (2013).
[9]S. K. Dwivedy and S. L. V. N. Avinash, Mech. Mach. Sci. **23**, 421 (2015).
[10]G. Y. Zhou and Q. Wang, Proc. SPIE **5760**, 226 (2005).
[11]S. Opie and W. Yim, J. Intell. Mater. Syst. Struct. **22**, 113 (2011).
[12]S. B. Choi, W. H. Li, M. Yu, H. P. Du, J. Fu, and P. X. Do, Smart Mater. Struct. **25**, 043001 (2016).
[13]M. A. Cantera, M. Behrooz, R. F. Gibson, and F. Gordaninejad, Smart Mater. Struct. **26**, 023001 (2017).
[14]Y. C. Li, J. C. Li, W. H. Li, and H. P. Du, Smart Mater. Struct. **23**, 123001 (2014).
[15]H. N. An, B. Sun, S. J. Picken, and E. Mendes, J. Phys. Chem. B **116**, 4702 (2012).
[16]I. A. Belyaeva, E. Y. Kramarenko, G. V. Stepanov, V. V. Sorokin, D. Stadler, and M. Shamonin, Soft Matter **12**, 2901 (2016).
[17]J. Nanpo, K. Nagashima, Y. Umehara, M. Kawai, and T. Mitsumata, J. Phys. Chem. B **120**, 12993 (2016).
[18]Y. Han, W. Hong, and L. A. E. Faidley, Int. J. Solids Struct. **50**, 2281 (2013).
[19]K. Danas, S. V. Kankanala, and N. Triantafyllidis, J. Mech. Phys. Solids **60**, 120 (2012).
[20]S. Rudykh and K. Bertoldi, J. Mech. Phys. Solids **61**, 949 (2013).
[21]M. R. Jolly, J. D. Carlson, and B. C. Munoz, Smart Mater. Struct. **5**, 607 (1996).